

# AN EMPIRICAL BASIS FOR EGS FLOW STIMULATION MECHANICS

Peter Leary<sup>1</sup>, Justin Pogacnik<sup>1</sup>, and Peter Malin<sup>1</sup>

<sup>1</sup>Institute of Earth Science and Engineering, University of Auckland, 58 Symonds Street, Auckland, New Zealand

p.leary@auckland.ac.nz

**Keywords:** *Fractures, fracture connectivity, lognormal distributions, well logs, well core, flow simulation*

## ABSTRACT

Population statistics of *in situ* permeability, trace element abundance, and ore grade data typically range from normal to long-tailed/lognormal distributions. A range of permeability statistics is simply expressed by  $\kappa = \kappa_0 \exp(\alpha(\varphi - \varphi_0))$ ,  $\kappa$  = permeability,  $\varphi$  = porosity (empirically normally distributed), with parameter  $\alpha$  ratioing the standard deviation of  $\log \kappa$  to the standard deviation of  $\varphi$ . For  $\alpha$  small, permeability is normally distributed in accordance with  $\varphi$ ; for  $\alpha$  large, permeability is manifestly long-tailed/lognormal,  $\log \kappa \sim \alpha \varphi$ . Relation by  $\kappa = \kappa_0 \exp(\alpha(\varphi - \varphi_0))$  derives from extensive well-log and well-core data. Well-log power-spectra scale inversely with spatial frequency,  $S(k) \sim 1/k$  over five decades  $\sim 1/\text{km} < k < \sim 1/\text{cm}$ , characterizing long-range spatially-correlated *in situ* grain-scale-density fluctuations. While grain-scale fracture densities are normally distributed, fracture-connectivity ranges from normal (low levels of connectivity) to lognormal (high levels of connectivity). Fracture connectivity ranges are attested by well-core poroperm data relating fluctuations in porosity  $\varphi$  to fluctuations in permeability  $\kappa$ ,  $\delta \varphi_j \sim \delta \log \kappa_j$ ,  $j = 1, \dots, N$ , for  $\delta \varphi_j$  and  $\delta \log \kappa_j$  = zero-mean/unit-variance fluctuation sequences of well-core porosity and  $\log(\text{permeability})$ . Naturally occurring fracture connectivity ranges in the crust thus explain the normal-to-lognormal range of statistical descriptions of well-core permeability, trace element abundance, and ore grade data. Expression  $\kappa = \kappa_0 \exp(\alpha(\varphi - \varphi_0))$  implies that for fixed porosity distribution  $\varphi$  increased permeability is associated with increased fracture connectivity of grain-scale fractures. Finite shear strain in a crustal volume inducing new grain-scale defects in association with existing grain-scale fracture porosity hence can create greater permeability through greater fracture connectivity. Naturally occurring finite-strain injection can explain the range of fracture-connectivity observed in normal-to-lognormal distributions for well-core permeability, trace element abundance, and ore body grades, from which we may infer that permeability enhancement for EGS heat-exchange volumes can be achieved through properly designed strain-damage-inducing wellbore pressurization.

## 1. BACKGROUND

The Ngawha geothermal outcrop near Lake Omapere in Northland is a highly accessible prototypal Enhanced/Engineered Geothermal System (EGS) resource. The site offers ten or so square kilometers of very shallow (500m) yet commercially hot ( $>200^\circ\text{C}$ ) low porosity (1-4%), low permeability basement (greywacke metamorphic) rock heated by molten intrusives below and insulated by impermeable sedimentary rock above (DSIR7 1981). The greywacke basement has good potential for fracture permeability development needed by EGS projects: moderate to good fracture permeability ( $>20$  Darcy-meter) at Ngawha in probable association with historic faulting (DSIR7), and documented greywacke fracture permeability

in the tectonically active Taupo Volcanic Zone (Wallis et al 2012). Active tectonics aside, *in situ* greywacke permeability appears likely to be that of metamorphic rock in general. The defining feature of EGS potential is learning how to engineer low permeability basement such as the Ngawha greywacke into permeable heat exchange volumes.

Ngawha's fortuitously shallow basement heat resource provides a natural EGS laboratory in which to explore for scientific/engineering means by which to control *in situ* fracture permeability. We advance here one such means based on evidence that *in situ* permeability is controlled by fracture-connectivity at all scale lengths. Abundantly attested well-log and well-core spatial fluctuation systematics indicate that *in situ* permeability is physically defined by percolation along naturally occurring, spatially erratic fracture-connectivity pathways on scales from mm to Km. The range of trace element and ore grade distributions in many rock types provide supporting evidence that spatially varying *in situ* permeability is due to spatially varying degrees of fracture connectivity at Dm-to-Km scales. We propose to focus on controlling *in situ* fracture connectivity in a crustal volume as a means to achieve commercial grade EGS-capable permeability.

The rewards for EGS capability are great. Potential base-load electrical power production for EGS sites worldwide far exceeds that of hydrothermal systems. Western US hydrothermal resources are estimated at 3.7GWe existing/known hydrothermal capacity (with potential for 7.9GWe), while EGS resources are estimated to be two orders of magnitude greater at 345GWe [USGS Fact Sheet 2008-3082]. EGS geothermal power resources are also far more widely geographically distributed than hydrothermal power resources limited to active extensional tectonic regions.

Despite the allure of large numbers, however, no attempts to realize EGS commercial power have succeeded. One, possibly the main, reason for past EGS failures may have been inadequate understanding of fluid flow mechanics in fractured rock. It is perhaps relevant to note that oil/gas reservoir modeling systematically overlooks fracture heterogeneity as a component of *in situ* flow, possibly in the belief that formation geological uniformity implies petrophysical uniformity. Industry practice (e.g., Earlougher 1977) that defines reservoir flow in terms of a single parameter ' $kh$ ' (the product of formation permeability  $k$  and height  $h$ ) argues for such a belief. While well-log spatial fluctuation data readily demonstrate its fallacy, the oil/gas industry business model continues to use a few spot core samples and associated spot-log data to infer the porosity and permeability of geological formations. For spot physical sampling of geological formations to be statistically accurate, formation physical property spatial fluctuations must be uncorrelated; i.e., the spectrum  $S(k)$  of spatial property fluctuations must have the same value at all spatial frequencies  $k$ ,  $S(k) \sim 1/k^0 \sim \text{const}$ . In fact virtually all well-log spatial sampling of rock physical property distributions

have spatial fluctuation power spectra that scale inversely with spatial frequency,  $S(k) \sim 1/k^1$  over five to six decades of scale length,  $\sim 1/\text{km} < k < \sim 1/\text{cm}$ .

Possible influence by the oil/gas industry indifference towards evidence for *in situ* fracture/flow heterogeneity in favor of a  $kh$  reservoir uniformity concept would explain the steady expectation that large-scale EGS fracturing would provide spatial sequences of regularly-spaced geometrically-discrete flow apertures (e.g., Tester et al 2006; Sutter et al 2011). The absence of such predictable wellbore-to-wellbore flow, and the highly disseminated microseismicity distributions generated by EGS fracture stimulation efforts at Fenton Hill/US and Rosemanowes/UK (Tester et al 2006), and recently at Paralana in South Australia (Reid et al 2011), does not support such fracture enhancement uniformity. Additionally, EGS projects appear to have largely ignored field contemporaneous evidence for pervasive large-scale fracture permeability heterogeneity in generic crustal rock first advanced by Brace (1980), then extended to a wide range of scales by Neuman (1990) and Clauser (1992), and subsequently by many others (e.g., Neuman 1994; Schulze-Makuck & Cherhauer 1995). The idea that EGS basement rock types systematically differ from oil/gas reservoir sedimentary rock types is easily refuted; it is clear that well-log spatial fluctuation systematics do not distinguish between the fracture spatial distribution properties of crystalline and sedimentary rock types (Leary 2002).

In light of scientific and engineering evidence against effective spatial uniformity for EGS crustal volumes, we turn to well-log and well-core spatial fluctuations evidence for systemic *in situ* fracture-induced permeability heterogeneity on all scales. In particular, well-log/well-core fluctuation empirics can explain the observed range of lognormality skewness in permeability, trace element abundance, and ore grade and ore body size distributions. Such lognormality skewness is traceable to varying degrees of fracture connectivity within *in situ* fracture networks: the greater the connectivity, the greater the lognormal skewness of permeability distributions, and the greater the overall fracture permeability. After briefly reviewing the *in situ* fracture empirics of crustal rock, we focus on this potential to enhance *in situ* permeability via controlled stimulation of fracture connectivity in EGS heat exchange volumes at Ngawha and elsewhere.

## 2. FRACTURE CONNECTIVITY AND *IN SITU* PERMEABILITY DISTRIBUTIONS

Three wellbore-based empirical rules appear to define the main aspects of *in situ* fluid flow mechanics. First, well-log data reveal a pervasive inverse power-law scaling rule for the physical-variable fluctuation Fourier transform power  $S(k)$  over five decades of spatial frequency  $k$ ,

$$S(k) \approx 1/k, \sim 1/\text{km} < k < \sim 1/\text{cm}. \quad (1)$$

Equation (1) holds for a wide range geological settings and geophysical variables, and for both horizontal and vertical wells (Leary 2002). The five-decade scale range runs from 1cm wellbore sampling of microresistivity logs to multiple-km sampling of spatial fluctuations in sonic velocity, neutron porosity, mass density, gamma activity and electrical resistivity.

Second, well-core data from oil/gas field clastic reservoir formations establish a close relation on the scale of cm to

dm between fluctuations in well-core porosity  $\phi$  and the logarithm of well-core permeability  $\kappa$ ,

$$\delta\phi \approx \delta \log(\kappa). \quad (2)$$

Eqs (1)-(2) can be jointly interpreted to mean that *in situ* fracture systems are spatially-correlated grain-scale-fracture-density networks through which *in situ* fluids can percolate on all scale lengths, with porosity having close spatial affinity to grain-scale density hence effectively controlling permeability through interconnectivity of grain-scale fractures (Leary 2002; Leary & Walter 2008).

Recasting (2) as an explicit relation between two zero-mean/unit-variance well-core sequences,

$$(\phi_i - \langle \phi \rangle)/\sigma(\phi) \approx (\log(\kappa_i) - \langle \log(\kappa) \rangle)/\sigma(\log\kappa), \quad i=1,\dots,n,$$

we can integrate the sequence of dm-scale fluctuations to give  $\log(\kappa) - \log(\kappa_0) = \alpha(\phi - \phi_0)$ , where  $\alpha \equiv \sigma(\log\kappa)/\sigma(\phi)$  ratios the standard deviations of well-core sequences  $\log\kappa$  and  $\phi$  respectively, and  $\phi_0, \kappa_0$  are minimum values for porosity and  $\log(\text{permeability})$  sequences with  $\log(\kappa_0) \equiv \min(\log\kappa)$ . Writing the integrated form as an exponential gives *in situ* permeability as an empirical function of *in situ* porosity controlled by empirical parameter  $\alpha$  over the Dm to Hm scale range,

$$\kappa \approx \kappa_0 \exp(\alpha(\phi - \phi_0)), \quad (3)$$

Empirically, porosity is almost always normally distributed physical variable with a tractable standard deviation and mean. If a porosity sequence is renormalized as a zero-mean, unit-variance variable  $n$ , and  $\mu$  is the median of the  $\log(\text{permeability})$  sequence, (3) corresponds to the mathematical definition of a lognormal distribution,

$$\kappa \approx \exp(\mu + \sigma n), \quad (3a)$$

with  $\sigma$  the lognormality skewness parameter. The median value of (3a) occurs at the median value of  $n$ , which is zero, hence  $\exp(\mu)$  is the median value of  $\kappa$ . The mean value of  $\kappa$  is  $\exp(\mu + \sigma^2/2)$  showing how parameter  $\sigma$  strongly controls the skewness or long-tailed character of lognormal distributions. The essential aspect of distributions (3) and (3a) is that many values are small while a few are large.

Populations (3) or (3a) with small skewness parameter  $\sigma$  are themselves normal distributions because the exponent expands to a term linear in  $\sigma n$ ,  $\exp(\sigma n) \approx 1 + \sigma n$ . Populations with large  $\sigma$  are highly skewed so that many small values occur for every large value. Because of the strong role played by spatial correlation (1) in the population of *in situ* grain-scale fractures, skewness  $\sigma$  takes on a physical role as proxy for spatial connectivity. Small spatial connectivity is thus associated with normally distributed permeability of limited magnitude (small  $\sigma n$  limit), while large spatial connectivity is associated with long-tailed permeability distributions with increasingly large net permeability. We hence establish that the *in situ* empirics (3) of wide ranges of lognormality in populations of well-core permeability, trace element abundances, and ore grade and ore body size are a manifestation of *in situ* fluid flow rules (1)-(2).

### 3 INTERPRETATION OF LOGNORMAL DISTRIBUTIONS IN *IN SITU* FLOW PROCESSES

Figs 1-2 illustrate the mechanics of fracture-connectivity control of fluid flow pathways and overall permeability in 2D realizations of crustal poroperm media following the empirics of (1)-(2). The 2D poroperm media are based on spatially-correlated porosity fluctuations throughout the medium, for which a well log through the medium returns a fluctuation spectrum scaling inversely with spatial frequency as (1). Permeability within the medium is associated with porosity by (2) and the degree of fracture connectivity by (3).

Fig 1 realizes a sequence of permeability distributions  $\kappa \approx \kappa_0 \exp(\alpha(\varphi-\varphi_0))$  associated with a fixed porosity distribution  $\varphi$  for an incrementing range of fracture-connectivity parameters  $\alpha$ . As  $\alpha$  increases, the permeability distributions become more skewed, and the overall permeability of the medium increases as greater fracture connectivity allows readier passage of fluid.

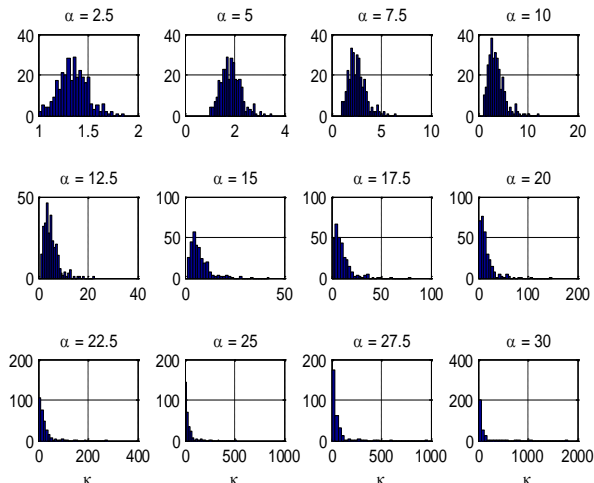


**Figure 1.** Permeability population distributions (3) for  $\kappa \approx \kappa_0 \exp(\alpha(\varphi-\varphi_0))$  for  $\alpha = 2.5$  to 30 for fixed normal porosity distribution  $\varphi$ . As  $\alpha$  increases, maximum permeability increases while the minimum permeability remain fixed, hence the frequency distribution becomes more ‘long-tailed’ (more lognormal).

Fig 2 realizes the fluid flow distributions associated with the range of permeability distributions. The left hand column displays a range of permeability distributions, from low skewness at the top to high skewness at the bottom. The central and right-hand columns display the pressure and velocity fields generated by fluid issuing from a central wellbore. The vertical sequence of pressure fields shows that pressure typically remains uniform to quasi-uniform about the central wellbore. This degree of uniformity is not, however, observed by the fluid velocity field. Rather the fluid flow becomes channeled by fracture connectivity that increases with increasing permeability distribution skewness. Along with increasing skewness, the net medium permeability increases as quantified by the left-hand column histograms. Flow simulation details are given by Leary & Malin (2011).

Figs 1-2 invite us to understand that flow phenomena such as solute and heat transport are markedly affected by fluid channelization, generating a range of trace element abundance and ore grade distributions that reflect a flow property duality of high flow channelization and high rates

of deposition. Beginning with an illustration of the range of well-core permeability distributions, evidence for such flow transport duality is presented in the following sections.

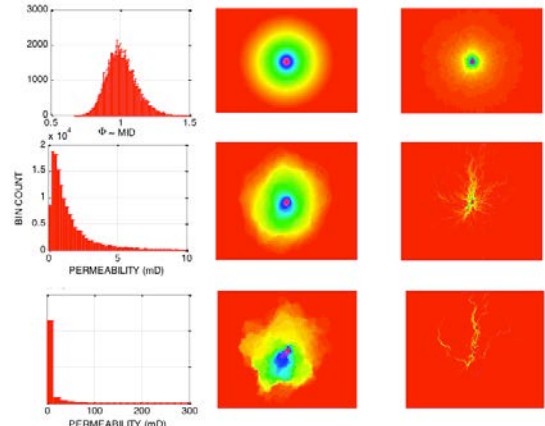


**Figure 2.** Growth of fracture-connectivity permeability for three increasing values of fracture-connectivity parameter  $\alpha$  in permeability distribution (3)  $\kappa \approx \kappa_0 \exp(\alpha(\varphi-\varphi_0))$ . Left column: Increase skewness of permeability distribution with increasing  $\alpha$ . Centre/right columns: pressure and fluid velocity distributions for fluid issuing from central wellbore into 2D poroperm media determined by (3). Upper row: small  $\alpha$  with little fracture connectivity. Centre/lower rows: increasing  $\alpha$  means increasing degrees of fracture-connectivity control of fluid pathways and greater overall permeability.

### 4. WELL-CORE PERMEABILITY DISTRIBUTIONS

A tendency for oil-field well-core permeability populations to be ‘long-tailed’ or ‘lognormally’ distributed has long been recognised (Law 1944; Bennion & Griffiths 1966; Freeze 1975; Dagan 1989). Figs 3-4 illustrate the range of lognormal skewness in the reservoir samples. The effective value of lognormality parameter  $\alpha$  is determined by plotting  $\log(\kappa)$  against porosity  $\varphi$ . Because additional factors affect sample porosities, the straightforward relation of Fig 2 between lognormality and  $\alpha$  is absent.

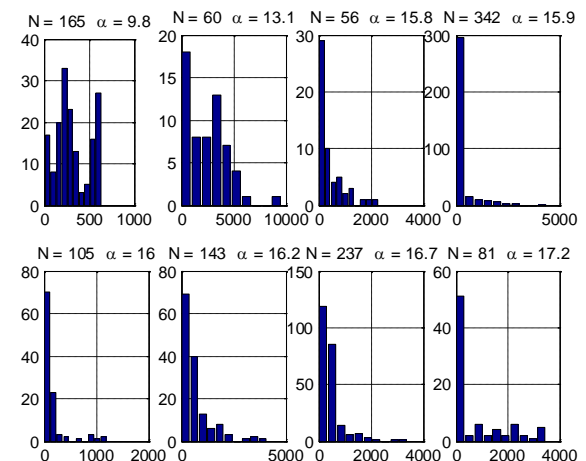


**Figure 3.** Permeability distributions from a North Sea clastic reservoir. Lower values of  $\alpha$  associate with more normal distributions and higher values of  $\alpha$  associate with longer-tailed distributions but additional factors complicate the relation.

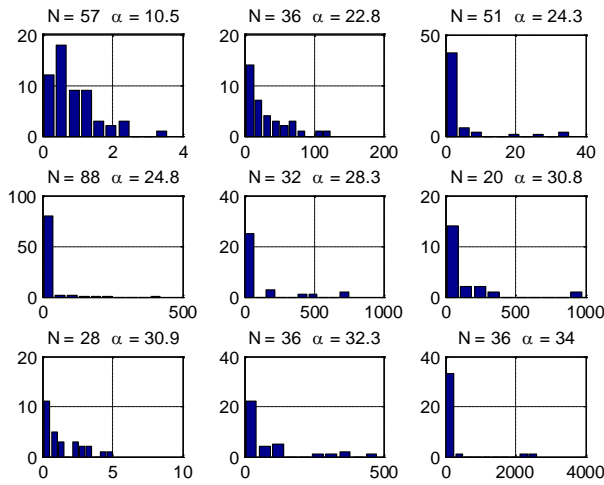


**Figure 4.** Permeability distributions from a South Australia clastic reservoir. As with Figure 3, other factors complicate the relation between measured  $\alpha$  and degree of lognormality.

The sample clastic formation well-core permeability data establish that lognormality is a common feature of reservoir rock. Empirical relations (1)-(3) relate lognormality to the presence of fractures. It is thus clear that, in contradistinction to standard industry assumption, fluid flow in reservoir rock is substantially influenced by the presence of fractures, and that in consequence fracture heterogeneity is likely to affect the production behavior of wells. The evidence below is that the same phenomenology is in play in metamorphic and igneous rock with more obvious affinity to EGS basement rock.

## 5. TRACE ELEMENTS DISTRIBUTIONS

The general picture of trace element distributions in largely igneous rock is that some are normal while a large number are lognormal (Ahrens 1954a, 1954b, 1957, 1963). Ahrens (1963) cites 32 instances of lognormal trace element distributions in granite against two of near-normal distribution; five instances are judged uncertain. A snapshot summary of aspects of Ahrens (1963) trace element distributions in Figs 5-6 visually connects with the poroperm distribution systematics illustrated in Figs 1-4. Figs 5 illustrates that a skewed trace element abundance distribution (left) is properly lognormal (right) because the distribution of the log(abundance) is Gaussian.

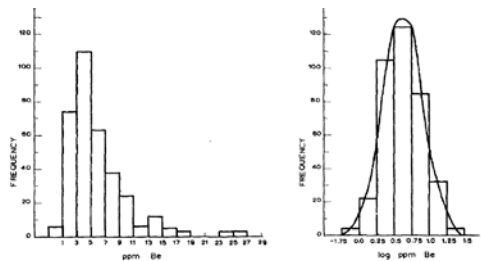


**Figure 5.** A trace element abundance distribution from Ahrens (1963) showing a lognormal distribution (left) and its normal log(abundance) distribution (right).

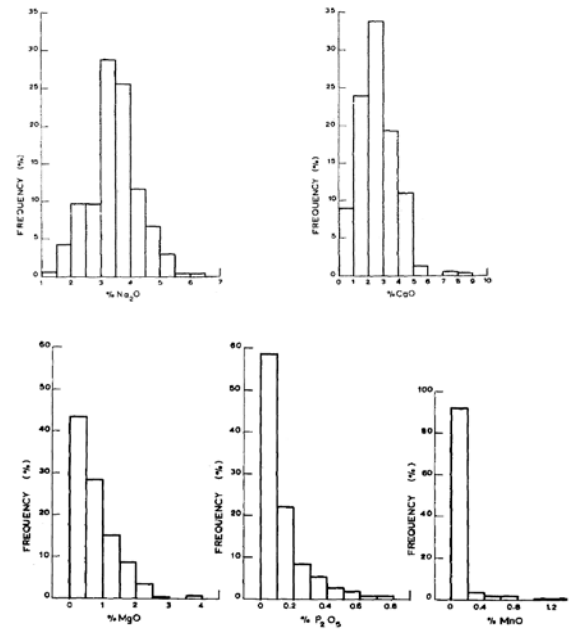
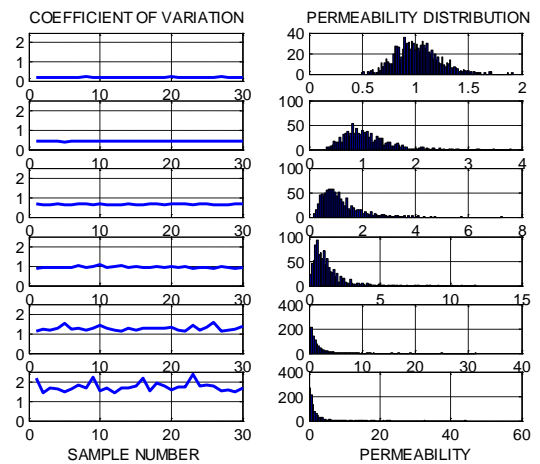


**Figure 6.** Five trace element abundance distributions from Ahrens (1963) grading from near-normal (top left) to 'lognormal' (bottom right).

Fig 6 illustrates a range of skewness for a sequence of trace element abundances in granite; the element abundances are for Na, Ca, Mg, P, and Mn.

## 6. ORE GRADE DISTRIBUTIONS

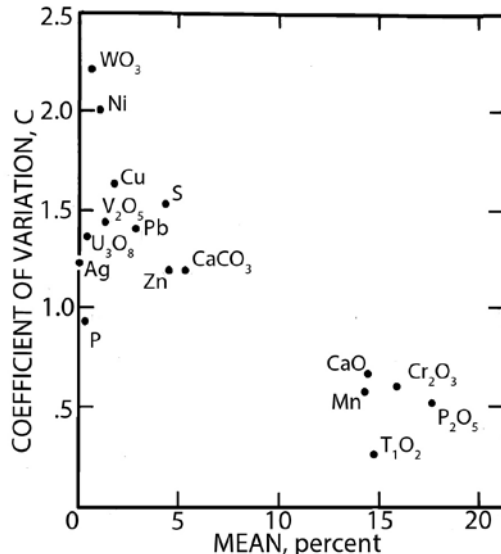
The ratio of the standard deviation to the mean of a population distribution, termed the 'coefficient of variation', is bounded by approximately  $1/2$  for the distribution to be normal or Gaussian. If the coefficient of variation is larger than  $\sim 1/2$  then the distribution can be lognormal.



**Figure 7.** (Left) Coefficient of variation for 30 realisations of permeability for a top-to-bottom sequence of increasing skewness parameter  $\alpha$  in (3). (Right) Representative permeability distributions for each value of  $\alpha$ , from quasi-normal (top) to highly skewed lognormal (bottom).

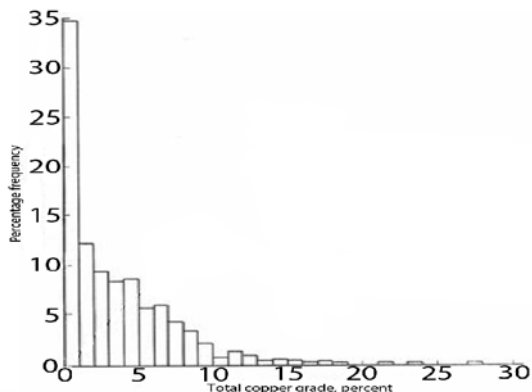
Fig 7 illustrates the coefficient of variation phenomenology in a sequence of realizations of poroperm distributions (3) for parameter  $\alpha$  increasing from top to bottom. The right

column shows the permeability distribution, from normal at top to lognormal at bottom; the left column shows that the coefficient of variation is uniformly below  $\frac{1}{2}$  for normal distributions, rising steadily above  $\frac{1}{2}$  to reach 2.5 as the distributions become more skewed. Fig 8 shows a range of coefficients of variation determined by Koch & Link (1971) from trace element abundance data compiled by Hazen & Meyer (1966) from nearly 500 mineral deposits. From Fig 7 it is seen that elements with low abundances have coefficients of variation consistent with lognormal abundance distribution.



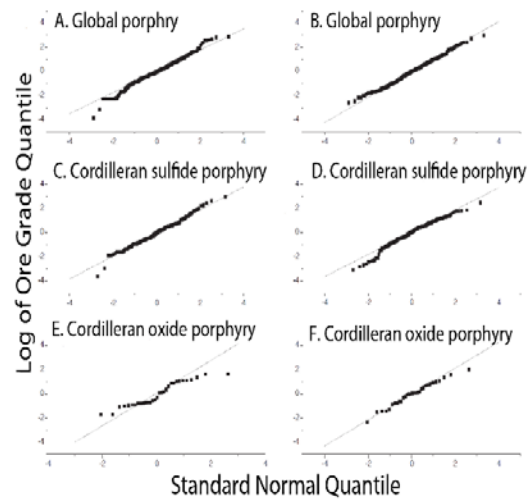
**Figure 8.** Coefficients of variation for ore deposit data (after Koch & Link 1971). Low abundance elements have high coefficient of variation values implying strongly lognormal abundance distributions – see Fig 7.

Fig 9 shows copper ore grade distribution data from Clark & Garnett (1974) to be lognormally distributed.



**Figure 9.** Histogram plot of copper ore grade data (after Clark & Garnett 1974).

In Fig 10, Gerst (2008) analyses copper ore distributions by comparing quartile distributions of log(Ore Grade) data from a range of deposits types against a standard Gaussian quartile distribution. The fact that log(Ore Grade) data plot on a straight line of unit slope against a Gaussian normal distribution means the ore grade data are lognormally distributed.



**Figure 10.** Plots of quartile distributions of log(Ore Grade) data on vertical axis against a standard Gaussian quartile distribution on the horizontal axis. The straight line of unit slope means the log(Ore Grade) data are Gaussian distributed, hence that ore grade distributions are lognormally distributed. Plot after Gerst 2008.

## 7. SUMMARY/CONCLUSION

Figs 3-10 review well-core distributions of permeability, trace element abundance, and ore grade distributions for rock types spanning oil/gas reservoir clastic sands, to metamorphic deposition systems, to reef systems, to igneous intrusions. In each case there is unambiguous evidence for lognormal distributions, often as the dominant feature. The general tenor of discussions accompanying the data is that lognormality is ‘the norm’ rather than a collection of statistical outliers. In each case it is plausible that the data reflect *in situ* fluid flow regimes leading to many instances of poor flow against a few instances of rich flow. This flow/deposit phenomenology is consistent with the flow systematics of Figs 1-2 and reprised in Fig 11 in the context of EGS.

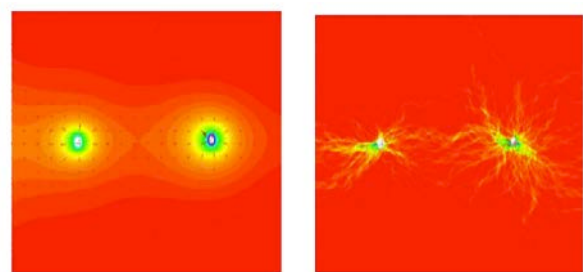


**Figure 11.** Wellbore-to-wellbore flow velocity distributions for degrees of fracture connectivity given by lognormality skewness parameter  $\alpha$  in (3). Flow in poroperm media with small skewness are essentially uniform flow media as often assumed for geological formations. Large skewness leads to to filamentary flow along spatially-organised long-range-correlated high permeability fracture-pathways. Evidence for lognormal distributions in reservoir rock, mineral deposition environments, and igneous intrusion favors the right-hand flow diagram as a model of *in situ* flow.

Fig 11 synopsizes the physical significance for EGS of well-log/well-core fluid flow empirics (1)-(3) and associated flow/deposit phenomenology of Figs 3-10. In a variation on Fig 2, Fig 11 contrasts two fluid velocity fields computed for 2D flow from an entry wellbore to an exit wellbore. High flow velocities near the wellbore (green), grade to lower velocities away from the wellbore (yellow to red). The left/right panels compare velocity fields for low/high value of fracture-connectivity parameters  $\alpha$  from (3). The change in fracture-connectivity for the poroperm medium produces a substantial difference in flow distribution, from a poroperm medium on the left resembling the oil/gas industry standard concept of quasi-uniform flow through a quasi-uniform permeability, to a quite different poroperm medium on the right that heavily involves fractures and fracture connectivity. We see that fluid flow spatial distributions in poroperm media conforming to empirical rules (1)-(2) are structurally controlled by lognormality skewness parameter  $\alpha$ , indicating that fracture connectivity within a population of grain-scale cement-defects permits and promotes large-scale percolation pathways through long-range spatially-correlated connectivity of grain-scale defects.

We further see that moderate to large lognormality skewness consistent with the right-hand diagram of Fig 11 is typical of hydrocarbon reservoirs and generally associated with significant trace element abundances and high grade ore bodies. The wide-spread nature of clastic reservoir well-core poroperm, trace element abundance, and ore grade distributions indicates that poroperm phenomenology (1)-(3) is a common feature of crustal rock. We infer that such fracture-connectivity phenomenology can likely be exploited in interest of EGS permeability enhancement. Pogacnik et al (2012) explore the detailed physics of this phenomenology.

We conclude from the above data and discussion that a likely statement of the object of EGS fracture connectivity enhancement is to move EGS heat exchange volumes from the left-hand side of Fig 11 to the right-hand side.

## REFERENCES

Ahrens LH (1954a) The lognormal distribution of the elements, I. *Geochim Cosmochim Acta* 5, 49-73.

Ahrens LH (1954b) The lognormal-type distribution of the elements, II. *Geochim Cosmochim Acta* 6, 121-131.

Ahrens LH (1957) Lognormal distributions, III. *Geochim Cosmochim Acta* 11, 205-212.

Ahrens LH (1963) Lognormal-type distributions in igneous rocks – IV, *Geochimica Cosmochim Acta* 27, 333-343.

Bennion DW & Griffiths JC (1966) A stochastic model for predicting variations in reservoir rock properties, *Soc. Petrol. Eng. Jour., Trans. ATME*, 237, 9-16.

Brace WF (1980) Permeability of crystalline and argillaceous rocks, *Int. J. Rock Mech. Min. Sci. & Geomech Abst* 17, 241-251.

Clark I & Garnett RHT (1974) Identification of multiple mineralization phases by statistical methods, *Trans. Inst. Min. Metall.*, Vol 83, pp.A43

Clauser C (1992) Permeability of crystalline rocks, *EOS Transactions AGU* 73 No 21, 233-237.

Dagan G (1989) *Flow and transport in porous formations*, Springer-Verlag, Berlin, 465 p.

Earlougher RC (1977) *Advances in Well Test Analysis*, Society of Petroleum Engineers, Dallas, pp264.

Freeze RA (1975) A stochastic-conceptual analysis of one-dimensional groundwater flow in nonuniform homogeneous media, *Water Resources Research* 11, No. 5, 725-741.

Gerst MD (2008) Revisiting the Cumulative Grade-Tonnage Relationship for Major Copper Ore Types, *Economic Geology* 103, 615-628.

Hazen SW & Meyer WL (1966) Using probability models as a basis for making decisions during mineral deposit exploration, US Bureau of Mines Report 6778, pp83.

Ingebritsen S, Sanford W & Neuzil C (2006) *Groundwater in Geological Processes*, Cambridge University Press, pp536.

Koch GS & Link RF (1971) The coefficient of variation; a guide to the sampling of ore deposits, *Economic Geology* 66, 293-301.

Law J (1944) A statistical approach to the interstitial heterogeneity of sand reservoirs, Technical Publication 1732, *Petroleum Technology* 7, May 1944.

Leary P & Malin P (2011) Is Theis flow modeling sufficient for EGS/HSA geothermal energy production? Geothermal Research Council, San Diego, 23-26 October 2011.

Leary PC & Walter LA (2008) Crosswell seismic applications to highly heterogeneous tight gas reservoirs *First Break* 26, 33-39.

Leary PC (2002) In: J.A. Goff & K. Holliger (Eds.) *Heterogeneity of the Crust and Upper Mantle - Nature, Scaling and Seismic Properties*, Kluwer/Academic/Plenum Publishers, New York, 155-186.

Pogacnik J, Leary P & Malin P (2012) Physical computational framework for EGS *in situ* fracture stimulation, Proceedings 34<sup>th</sup> New Zealand Geothermal Workshop, Auckland, 19-21 November.

Neuman SP (1990) Universal scaling of hydraulic conductivities and dispersivities in geologic media, *Water Resources Research*, 26 p1749.

Neuman SP (1994) Generalized scaling of permeabilities: Validation and effect of support scale, *Geophys. Res. Lett.* 21, 349-352.

Reid PW, Messeiller M & Llanos EM (2011) Paralana EGS Project –Findings from the fracture stimulation, *Proceedings Australian Geothermal Energy Conference*, Melbourne, 17-19 November.

Schulze-Makuck D & Cherhauer DS (1995) Relation of hydraulic conductivity and dispersivity to scale of measurement in a carbonate aquifer, In: Models for Assessing and Monitoring Groundwater Quality, ed. By B.J. Wagner, T. H. Illangasekare & K. H. Jensen, IAHA Publication No. 227.

Sutter D, Fox DB, Anderson BJ, Koch DL, von Rohr PR & Tester JW (2011) Sustainable heat farming of geothermal systems: a case study of heat extraction and thermal recovery in a model egs fractured reservoir. *Proceedings 36<sup>th</sup> Workshop on Geothermal Reservoir Engineering*, Stanford University, January 31-February 2.

Tester JW et al (2006) The Future of Geothermal Energy, <http://geothermal.inel.gov>  
[http://www1.eere.energy.gov/geothermal/egs\\_technology.html](http://www1.eere.energy.gov/geothermal/egs_technology.html)